

Prediction of nonlinear distortion of HTS filters for CDMA communications systems

C.Collado, J.Mateu, R. Ferrús, J.M.O'Callaghan

Abstract— HTS materials are known to produce intermodulation and other nonlinear effects, and this may restrict their use in wireless communication systems. While significant efforts are being done to measure and characterize nonlinear properties of HTS materials, there are very few works that relate these properties to system parameters. In this work we attempt to bridge this gap by analysing the nonlinear performance of a superconducting RF front-end for Third-Generation Mobile Communications Systems. We assume that a quasi-elliptic pre-select HTS filter is used as the first device in the receiver chain, and we analyse its performance using Harmonic Balance algorithms. The compliance of UMTS specifications for system parameters like Adjacent Channel Power Ratio (ACPR), AM-AM and AM-PM distortion, error vector magnitude (EVM), is assessed in various environments.

Keywords— Nonlinearities, CDMA, HTS filters

I. INTRODUCTION

Third-generation (3G) wireless systems are designed for multimedia applications, where person-to-person communication and/or access to information and services on public and private networks will be enhanced by the higher data rates. 3G are based on spread spectrum techniques where the different code division multiple access (CDMA) signal users are multiplexing onto the same frequency channel using Orthogonal Variable Spreading Factor (OVSF) and gold-code scrambling.

In dense electromagnetic environment with high data rates, filtering is an essential feature to consider only the desired frequency band and maintain these data rates. The low RF losses of High Temperature Superconductor (HTS) allows to achieve high performance passband filters. Unfortunately, HTS at microwave frequencies exhibit a nonlinear power dependence, even at moderated power levels, which usually involve dependence in the penetration depth on the current density. These nonlinear effects in HTS filters are distributed along the structure and can degradate the performance of the whole transceptor [ref].

In previous works we have proposed numerical techniques based on Harmonic Balance (HB) to predict the nonlinearity in a HTS resonator or filter, by quantifying one- or two tone response or power degradation [referencies]. However since the nonlinear response in spread spectrum modulated RF signals depends not only on the intrinsic nonlinearities, but also on the encoding method and modulation format being used [ref], the nonlinearities in CDMA signals are not completely quantify with one- or two tone response, so other parameters such as spec-

The authors are with the Dpt, of Signal Theory and Communications, Universitat Politècnica de Catalunya, Barcelona, Spain. E-mail: joano@tsc.upc.es

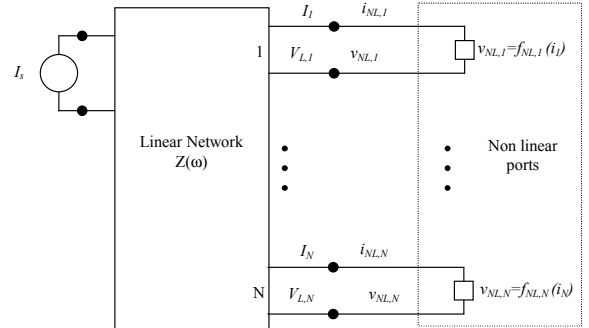


Fig. 1. Equivalent circuit of a nonlinear device consisting of a linear network with N+1 ports loaded with N nonlinear 1-ports.

tral regrowth or ACPR (Adjacent Channel Power Ratio), EVM (Error vector magnitude) or Eb/No (Bit energy noise density ratio) [ref] are necessary to estimate the nonlinear distortion in a real 3G communication system.

In this work we have extended the flexibility of the numerical technique based on HB to simulate signals with many frequency component like those of CDMA systems. We call this method Multitone Multiport Harmonic Balance (MMHB). We will present illustrative examples which show the viability of this kind of analysis for HTS frontend receivers and transmitters in 3G systems

Simulador made in home. Diagrama de bloques: (Señal WCDMA)+Amp+Filtro HTS. (Escenario WCDMA)+Filtro HTS+LNA. (amplificador no lineal simplificado). Flexible a filtros con diferentes topologías y tecnologías. y a difrenetes escenarios reales: intersystem (TDD-FDD) e interoperador (Near-Far)

II. MULTITONE MULTIPOINT HARMONIC BALANCE

Harmonic Balance is a common technique for the analysis of nonlinear microwave devices [ref]. Common to all HB algorithms is the splitting between the linear part, characterized in frequency-domain, and the non linear one, characterized in time-domain (Fig.1)

The linear part is characterized by its impedance matrix (\mathbf{Z}) of the (N+1)-port, where N ports are loaded with nonlinear elements and the remaining one is fed by a source. This matrix relates the voltage dropped along the N ports (V_L) and the current flowing out of the nonlinear network (I_L), which is impressed on the N nonlinear elements, and this matrix \mathbf{Z} has to be found at each input frequency component and all other frequencies where spurious signals may exist.[ref Journal] The nonlinear elements repre-

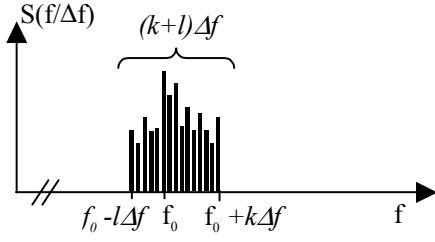


Fig. 2. Fourier Transform of $s(t)$

sent each small section which discretize the HTS filter [ref] and other nonlinear lumped elements of the frontend chain, such as amplifiers. In the nonlinear elements corresponding to the HTS device the relation between the current flowing through the nonlinear elements (I_{NL}) and the voltage (V_{NL}) is determined in time domain for each nonlinear port by

$$v_{NL}(i_{NL}) = \Delta R(i_{NL})i_{NL} + \frac{d}{dt}(\Delta L(i_{NL})i_{NL}) \quad (1)$$

where the nonlinear terms $\Delta R(i_{NL})$ and $\Delta L(i_{NL})$ can be derived from the properties of the material and the structure of each section in which the device is divided [ref, Dahm, balam disk, tim disk, asc2002 cav].

As detailed in previous work [Journal, tesi carlos], HB algorithm is based on an iterative procedure which match the voltage and current variables of the linear (V_L and I_L) and nonlinear part (V_{NL} and I_{NL}). The coexistence of the frequency-domain and time-domain equivalent current and voltage waveforms cause the necessity to convert between these domains by applying some kind of transformation (for a review see [Borich]) like a fast fourier transform (FFT).

A. Time-to-frequency and frequency-to-time conversion.

In 3G systems, the narrowband input signal consists of many closely spaced (Δf) frequency components, and can be write as:

$$s(t) = \text{Re} \left\{ \sum_{i=-l}^{i=k} a_i e^{j2\pi(f_0 + i\Delta f)t} \right\} \quad (2)$$

which results in a signal of bandwidth $BW = (k + l)\Delta f$. Note that the frequency resolution Δf is fixed by the window time of the input signal taken for the analysis $0 < t < T_0$, $\Delta f = 1/T_0$, [ref processat]. Fig 2 shows the fourier transform (TF) of eq. (2).

Throught the nonlinear system the resulting signal is a waveform with a larger number of closely spaced mixing products grouped at integer multiples of the center frequency (f_0) being $f_0/\Delta f \gg 1$,

$$y(t) = \sum_{n=0}^N \text{Re} \left\{ \sum_{v_{qn}} b_{qn} e^{j2\pi(v_{qn} + n f_0)t} \right\} \quad (3)$$

where v_{qn} denote new frequency components generated by the mixing products of the $k + l$ input frequency components and N is the order of the nonlinearites. To make the

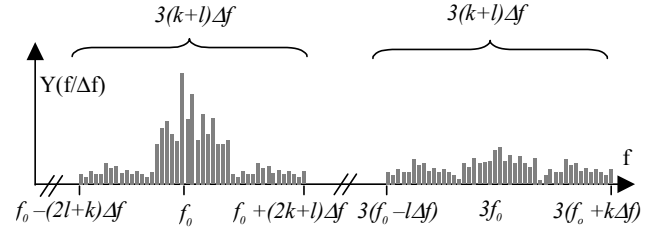


Fig. 3. Fourier Transform for the output signal $y(t)$. The location of the frequency components is set in eq. ()

formulation more understandable, we follow the expansion with the restriction of odd-nonlinearity and truncated at 3th order. In this case the frequency components of the output signal, $\kappa_{q,n} = v_{qn} + n f_0$, should satisfy [ref Borich]

$$\kappa_{q,n} = [[f_0 - (2l + k)\Delta f, \dots, f_0, \dots, f_0 + (2k + l)\Delta f], [3(f_0 - l\Delta f), \dots, 3f_0, \dots, 3(f_0 + k\Delta f)]]$$

and we can write eq.(3) as

$$y(t) = \text{Re} \left\{ \sum_{\kappa_{qn}} b_{qn} e^{j2\pi\kappa_{qn}t} \right\} \quad (5)$$

Figure 3 depicts the spectral distribution of the output signal.

Therefore, if we want analyze the spectrum shows in Fig.3 standard FFT techniques for spectrum determination require an impractically large number of time samples. However, since the signal is band-limited it is possible to locate the input signal to lower frequencies without losing information by choosing a relatively small sampling rate [ref].

As known from signal processing basics, e.g. [ref], the process of sampling (e.g., with a sampling rate of $f_s = 1/T_s$) is regarded as multiplication by an impulse train. Then by taking the FT of the sampled signal a sum of infinite original spectrum signal frequency-shifted is obtained. Now taking into account the frequency components of eq. (3) specied in eq (4) we set the conditions to fulfill by the sampling rate, f_s , to avoid overlapping effects, as

$$\begin{aligned} f_0 - p f_s &> (2l + k)\Delta f \\ f_s &> 3(l + k) \cdot 2 \cdot 2\Delta f \end{aligned} \quad (6)$$

where p is integer. Note that lower part of eq. (6) is set by the Nyquist condition [ref proc], where the output signal bandwidth is $3(l + k) \cdot 2\Delta f$, see Fig. 3 In practical applications we relaxed the conditions above, eq.(6), imposing:

$$\begin{aligned} f_0 - p f_s &> \varepsilon(2l + k)\Delta f \\ f_s &> \varepsilon 3(l + k) \cdot 2 \cdot 2\Delta f \end{aligned} \quad (7)$$

where $\varepsilon > 1$, and is necessary since the CDMA signals are not strictly band limited, and also because of the distributed nonlinear nature in HTS devices. These produce a

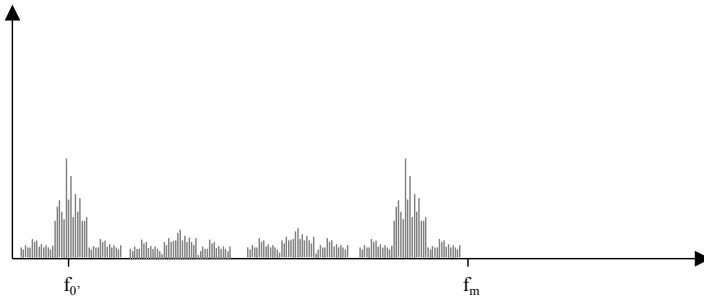


Fig. 4. Fourier Transform of $y_l(t)$ obtained by sampling $y(t)$ according to eq.(7)

wider regrowth than pointed out in eq (3). We also should notice these conditions are restricted to 3th order nonlinearities. For higher orders we can extract analog conditions on the sampling rate by following the procedure above.

From the sampled signal a location version of the original one can be written as

$$y_l(t) = \sum_{n=0}^N \text{Re} \left\{ \sum_{v_{qn}} b_{qn} e^{j2\pi(v_{qn} + n f_{0'})t} \right\} \quad (8)$$

where $f_{0'}$ is the lower frequency which satisfy, $f_{0'} = f_0 - p f_s$. Analogous to eq (4) we determine the position of the mapped coefficients, as

$$d_{q,n} = [[f_{0'} - (2l + k)\Delta f, \dots, f_{0'}, \dots, f_{0'} + (2k + l)\Delta f], [3(f_{0'} - l\Delta f), \dots, 3f_{0'}, \dots, 3(f_{0'} + k\Delta f)]] \quad (9)$$

In Fig.(4) are depicted the spectrum componets of eq (8). Note that spectrum coefficients are the same than Fig (3) located at d_{qn} positions.

Up to now we have demanstrate that it is possible to convert between time to frequency domain or viceversa working with an undersampling signal without losing information provided that the sampling rate, f_m , is properly chosen

At this point and before stepping up on the expansion, let us set some practical considerations for the analysis of the linear part of the problem, characterized by Z matrix

One of the most restrictive limitation of the simulations with the method propose will be the size of Z matrix. Its size depend directly on the number of nonlinear cells [ref HB] and also of the number of frequency components to define the matrix. Since the frequency components centered at multiples of f_0 are out of the harmonics of the HTS filter, the effects of these components on the ones inside the band of interes (centered al f_0), due to the nonlinearities, will be vanish. Then we only characterize Z at $[f_0 - (2l + k)\Delta f, \dots, f_0, \dots, f_0 + (2k + l)\Delta f]$, upper line of eq (4). This does not change the restriction on the sampling rate in order that the frequency components centered at $3f_0$ should not overlap on the in-band components.

The next step is to ensure that the nonlinear effects on the undersampled signal allow us to find the nonlinear effects unsampled one. To do this, firstly, let us consider the

resistive term of the nonlinear dependence eq. (1). Since this term presents a memoryless nonlinearity, the distortion effects in each sample-time just depends on sample-time itself so if the location fulfills the restrictions of eq.(7) we can obtain the waveform signal of the original nonlinear signal by relocating the coefficients from d_{qn} to κ_{qn} . On the other hand, the nonlinear inductive term represents a memory nonlinearity meaning the nonlinear effect in each sample-time depends on the past history or derivative information.

For the analysis of this memory term will be interested to express $y(t)$ and $y_l(t)$, eqs. (3) and (8), as a Fourier exponential serie (FES) expansion [ref], obtaining :

$$y(t) = \sum_{-\kappa_{qn}, \kappa_{qn}} \beta_{qn} e^{j2\pi\kappa_{qn}t} \quad (10)$$

$$y_l(t) = \sum_{-d_{qn}, d_{qn}} \beta_{qn} e^{j2\pi d_{qn}t} \quad (11)$$

respectively, where β_{qn} are the FES coefficients of $y(t)$ and $y_l(t)$. Since $y(t)$ and $y_l(t)$ are real signals its FES coefficients must fulfill $\beta_{qn} = \beta_{qn}^*$, and from eqs.(3) and (10) or eqs.(8) and (11) $\beta_{qn} = b_{qn}/2$.

Hence from eqs. (10) and (11), we obtain the derivative of $y(t)$ and $y_l(t)$, as:

$$\frac{dy(t)}{dt} = \sum_{-\kappa_{qn}, \kappa_{qn}} j2\pi\kappa_{qn}\beta_{qn} e^{j2\pi\kappa_{qn}t} \quad (12)$$

$$\frac{dy_l(t)}{dt} = \sum_{-d_{qn}, d_{qn}} j2\pi d_{qn}\beta_{qn} e^{j2\pi d_{qn}t} \quad (13)$$

Locating $d[y(t)]/dt$ to $f_{0'}$ it is obtained:

$$\left. \frac{dy(t)}{dt} \right|_l = \sum_{-d_{qn}, d_{qn}} j2\pi\kappa_{qn}\beta_{qn} e^{j2\pi d_{qn}t} \quad (14)$$

Note that the located signal derivative, eq. (13) , is not equal to the derivative signal located, eq. (14). To overcome this issue we work with the FT located signal thus multiplying frequency-domain signal by $j\omega$ (where $\omega = 2\pi\kappa_{qn}$) we find the derivative.

$$\frac{dy_l(t)}{dt} = \sum_{-d_{qn}, d_{qn}} j2\pi\kappa_{qn}b_{qn}e^{j2\pi d_{qn}t} = \left. \frac{dy(t)}{dt} \right|_l \quad (15)$$

Hence, we have demonstrate it is possible to analyze the many frequency components response throught distributed nonlinear devices by undersampling the input signal, even though working with memory nonlinearity terms.

B. Summary

The following summarize the steps involved in the application of the whole algorithm

Step 1: From the input signal frequency components, eq(2), and the order of the nonlinearities, eq(1), calculate

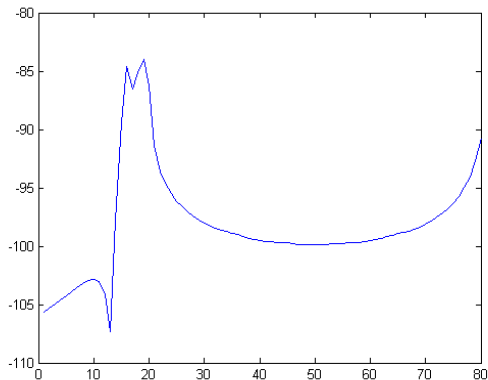


Fig. 5.

the new frequency components that we must take into account to keep all the information, e.i eq(4).

Step 2: Calculation of $Z(\omega)$ for the frequency components determined in step 1.

Step 3: By applying conditions outlined in eq(7), determine the frequency location $f_{0'}$ and the frequency sampling f_m to avoid overlapping effects. Straightforward from $f_{0'}$, f_m and κ_{qn} we find located position of the frequency components d_{qn} , e.i eq(9).

Step 4: Start with the HB algorithm (see Fig 3 of [Journal] and Fig. 1)

a) Propose a solution i_{NL} like the resulting located signal, eq(4).

b) Apply i_{NL} to eq(1) for each nonlinear port obtaining v_{NL} . Note that previously we should have calculated the derivative of the located signal in frequency domain by applying eq(15).

c) Transform v_{NL} to frequency domain and relocated the coefficients ($d_{qn} \Leftrightarrow \kappa_{qn}$).

d) Solve the linear part of the circuit by applying Z to find I_{NL}

e) Located I_{NL} coefficients to d_{qn} position and transform to time domain, resulting i_{NL} .

f): If the resulting signal of e) is not sufficiently close to the one propose in a), repite step 4 with a refined estimate solution.

III. EXAMPLES

In this section, we illustrate some commercially relevant application of the algorithm.

Petita introducció de les possibilitats del mètode.

Indicar quines no linealitats utilitzarem.

Indicar les diferents topologies de filtres a utilitzar i com em trobat les no linealitats per les diferents línies

A. Transmitter

SFDR: Escombrat en freq del SFDR, cal indicar diferents topologies, ordres i amplitud de banda

Figure que mostra per una part els regrowth a l transmetre una senyal: indicar potencia i els parametres de la

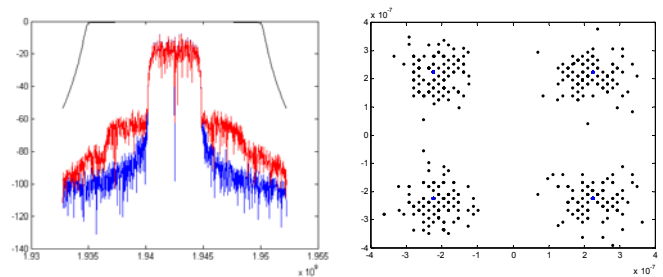


Fig. 6.

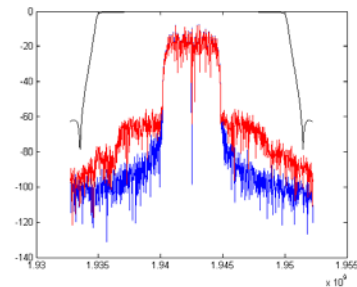


Fig. 7.

modulació i també les característiques del filtre. Al costat un figura amb EVM, també indicar potencia, modulacio, numero de bits, topologia del filtre.

Destacar que la figura anterior mostra per un banda els efectes de les no linealitats out-band i in-band

Introduir la taula que farem per tal de il·lustrar encara millor les utilitats d'aquesta eina de simulació

Tabla ACLR, IP3

Order	BW _{filter}	Top	Lin/Disk	SFDR	ACLR
12	5	CH	Lin		-1.1
12	15	CH	Lin		-7.65
12	5	QE (1.2)	Lin		-0.87
12	15	QE (1.2)	Lin		-8.62
12	5	CH	Lin		-10.32
12	15	CH	Lin		-16.39
12	5	QE (1.2)	Lin		-12.79
12	15	QE (1.2)	Lin		-17.07
8	5	CH	Disk		-18.44
8	15	CH	Disk		-21.37
8	5	QE (1.2)	Disk		-19.84
8	15	QE (1.2)	Disk		-21.48

Figure 4: Figura amb no linealitats d'amplificador, amplificador+HTSnonlinear filtre, amplificador+HTS filtre: parametres de la simulació i comentar els resultats obtinguts

B. Receiver

Intersystem and near far interferences: indicar el sistema que estem modulant, coemplacament, potencia de la senyal interferent, que teoricament no es poden fer aquest emplaçament, aïllament d'antena etc...

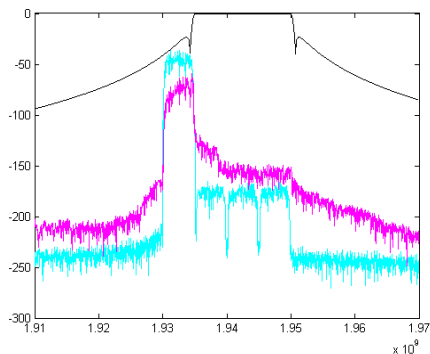


Fig. 8.



Fig. 9.

Gráfica con Eb/N0 para diferentes usuarios en función de la potencia Near far on Near Far, ja veurem

IV. CONCLUSIONS

This sample article has presented the style file `IEEEtran.cls`. This file can be especially useful in preparing articles for submission and for preparing the final version to be sent to the IEEE publishers.

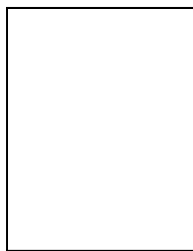
In essence, the style file “`IEEEtran.cls`” is not really for formatting (paper printout) – but is for IEEE *input processing* which is chalk and cheese, frankly.

ACKNOWLEDGMENTS

The authors would like to acknowledge the suggestions of many people.

REFERENCES

- [1] Leslie Lamport, *A Document Preparation System: L^AT_EX, User's Guide and Reference Manual*, Addison Wesley Publishing Company, 1986.
- [2] Helmut Kopka, *L^AT_EX, eine Einführung*, Addison-Wesley, 1989.
- [3] D.K. Knuth, *The T_EXbook*, Addison-Wesley, 1989.
- [4] D.E. Knuth, *The METAFONTbook*, Addison Wesley Publishing Company, 1986.



Gerry Murray will process your compuscript, adding “value” to your L^AT_EX file using a sophisticated text editor. Jeremy Barth will standardize the dimensions you've used, run a spell check, apply SGML tags to structure your document and validate all coding. The editor will “on-screen edit” the file, “size” your artwork and supply you with a laser proof by mail, or by fax, or even e-mail you a postscript version of the file which you can view on your workstation (using OpenWindows, NeXT, or an appropriate postscript viewer). When the editor is finished incorporating your amendments, Tom Bontrager, Mark Pheffer, Dalton Patterson or Chaucer Tran will receive the file and apply their abundant knowledge of typesetting to produce a document of the highest possible quality. A postscript file will be generated, output at 2032dpi on high quality RC paper for final examination by the editor. Christine will incorporate the artwork, the resulting camera-ready-copy will then be shot, the film supplied to the printer and your paper printed in the transaction for all to admire.